

Microwave Spectrum of $(\text{SiH}_3)_2\text{X}$, $\text{X} = \text{O}, \text{S}$, r_0 -Structure, Molecular Electric Dipolemoment and Barrier to Internal Rotation of Disilylsulfide

K. F. Dössel and D. H. Sutter

Abteilung Chemische Physik im Institut für Physikalische Chemie,
Christian-Albrechts-Universität Kiel

Z. Naturforsch. **33a**, 1190–1196 (1978); received July 28, 1978

The rotational spectrum of $\text{SiH}_3\text{—S—SiH}_3$ in its vib-torsional ground state has been investigated in the frequency range between 8 and 40 GHz. From the absolute frequencies and torsional splittings a rigid-top-rigid-frame r_0 -structure could be derived. The molecular electric dipole moment was determined from the second order Stark effect of some AA-species rotational transitions. The analysis of the microwave spectrum of the related molecule $\text{SiH}_3\text{—O—SiH}_3$ was yet unsuccessful. However several features of the observed spectrum lend support to the idea of a “quasi-linear” double rotor molecule with a relatively low energy hump for the linear configuration of the Si—O—Si-chain.

Introduction

Over the past years considerable effort has been put into the analysis of the microwave spectra of a group of “two top molecules”, having the general formula $(\text{CH}_3)_2\text{X}$ with $\text{X} = \text{O}$ [1], S [2] and Se [3]. From this work we have information on the structure, on the electric dipole moment, and on the barrier to internal rotation for these molecules. In the following we report the results of an investigation of the microwave spectra of the homologous silyl compounds $(\text{SiH}_3)_2\text{O}$ and $(\text{SiH}_3)_2\text{S}$, which was started with the aim to provide experimental data as a basis for a discussion of the bonding situation and of the origin of the barrier to internal rotation.

Experimental

The spectra were recorded with a conventional Stark-modulated (33 kHz zero based square wave) microwave spectrometer equipped with a brass waveguide cell of 8 m length and an inner cross section of 1 by 5 cm. Phase stabilized backward wave oscillators were used as radiation sources. Under typical recording conditions sample pressures were about 10 mTorr at temperatures around -65°C .

Disiloxane

A sample of $(\text{SiH}_3)_2\text{O}$ was obtained from Dr. A. Almendingen (Oslo). Once admitted to the cell, its microwave spectrum did not change in the course of a day. It was recorded in the frequency range from 23 to 40 GHz. Within the frame of the

standard rigid top-rigid frame model [4] and under the assumption of a Si—O—Si bond angle of about 145° as suggested from the electron diffraction work [5] one would expect to find the lower J -lines of the strong $1_{01} \rightarrow 1_{10}$, $2_{02} \rightarrow 2_{11}$, ... b -type Q-branch to fall into this frequency range. One would further expect, that the rotational spectra of molecules in the AA-torsional ground state of the SiH_3 -torsion should approximately follow a rigid rotor pattern with a second order Stark-effect, requiring higher Stark fields (i.e. E_{Stark} on the order of 1000 V/cm) for full modulation. However the search for this Q-branch of the AA-species failed. Although a great number of strong absorption lines were observed in the recorded range, all of them were fully modulated at Stark fields as low as 50 V/cm with unresolved low intensity Stark patterns, which indicates, that they all were high J transitions. To our opinion this result gives some support to the idea of a quasi-linear heavy atom chain with a comparatively low hump for the linear configuration, as was recently concluded from the Raman spectrum [6]. In such a molecule only vibration-rotation spectra would be allowed with selection rules $\Delta J = 0, \pm 1$; $\Delta v = \pm 1$, $\Delta l = \pm 1$ (v, l = quantum numbers for the bending vibration). With a vibrational energy gap of about 250 GHz [6] for

$$(v_{11} = 0, l_{11} = 0) \rightarrow (v_{11} = 1, l_{11} = \pm 1)$$

(the index “11” denotes the Si—O—Si bending vibration), the above mentioned “Q-branch frequencies” should be shifted approximately by this amount, which would explain the failure of our search. Although we have not yet been able to



Dieses Werk wurde im Jahr 2013 vom Verlag Zeitschrift für Naturforschung in Zusammenarbeit mit der Max-Planck-Gesellschaft zur Förderung der Wissenschaften e.V. digitalisiert und unter folgender Lizenz veröffentlicht: Creative Commons Namensnennung-Keine Bearbeitung 3.0 Deutschland Lizenz.

Zum 01.01.2015 ist eine Anpassung der Lizenzbedingungen (Entfall der Creative Commons Lizenzbedingung „Keine Bearbeitung“) beabsichtigt, um eine Nachnutzung auch im Rahmen zukünftiger wissenschaftlicher Nutzungsformen zu ermöglichen.

This work has been digitalized and published in 2013 by Verlag Zeitschrift für Naturforschung in cooperation with the Max Planck Society for the Advancement of Science under a Creative Commons Attribution-NoDerivs 3.0 Germany License.

On 01.01.2015 it is planned to change the License Conditions (the removal of the Creative Commons License condition “no derivative works”). This is to allow reuse in the area of future scientific usage.

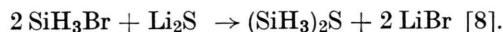
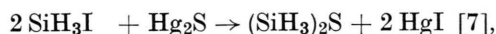
22767.7	31597.0
23020.9	32481.3
24668.3	33730.6
25078.2	34486.3
26668.8	35496.8
27249.3	36457.3
28632.9	37435.0
29254.2	38561.0
30661.5	40328.3

Table 1. Selection of very strong lines in the microwave spectrum of Disiloxane, (SiH₃)₂O (in MHz). All are fully modulated at Starkfields of 50 V/cm. For a complete list of recorded transitions see Ref. [19].

assign the more than 200 observed absorption lines, we list several strong lines for identification purposes in Table 1.

Disilysulfide

Initially we prepared samples of Disilysulfide by two different ways:



The second reaction turned out to be superior to the first, since it gave better yields and avoided the use of expensive iodine and poisonous mercury salts. Because (SiH₃)₂S readily reacts with water to form (SiH₃)₂O and H₂S, great care had to be taken, to remove traces of water adsorbed at the walls of the waveguide cell. Despite these precautions, the sample slowly decayed in the cell and after about two hours its spectrum became obscured by the much stronger lines of the (SiH₃)₂O spectrum (compare Table 1). Among the many lines belonging to either the (SiH₃)₂S or (SiH₃)₂O spectra, there also appeared some other very strong, unidentified lines, which might belong to the SiH₃SH molecule. To obtain the pure spectrum of (SiH₃)₂S the cell was refilled every hour.

The assignment of the spectrum was reported in a previous note [9]. In the following we present a refined analysis which includes centrifugal distortion effects. It is based on the effective rotational Hamiltonian given in Equation (1). This Hamiltonian may be thought of as the result of a second order perturbation treatment within torsio-vibrational states, i.e. a Van Vleck transformation, aiming at the vibrational and torsional groundstate. It is assumed that those matrixelements of the full Hamiltonian which are simultaneously off-diagonal in the torsional and vibrational quantum numbers are sufficiently small to justify their neglect, so

that the resulting effective rotational operator may be written as a blend of the standard PAM-Hamiltonian [4, 10] used for molecules with two top internal rotation and of the standard centrifugal distortion Hamiltonian [11] used for asymmetric top molecules.

$$\mathcal{H}_{v_1, \sigma_1, v_2, \sigma_2} = \mathcal{H}_r + F \sum_{i=1}^2 \sum_{n=1}^4 W_{v_i, \sigma_i}^{(n)} \mathcal{P}_i^n + \sum_{i=1}^2 W_{v_i, \sigma_i}^{(d)} \mathcal{H}_{iD} \quad (1a)$$

$$+ \mathcal{H}_{CD}. \quad (1b)$$

The symbols have the following meaning:

$v_1, \sigma_1, v_2, \sigma_2$ = internal rotation quantum numbers.

$$\mathcal{H}_r = A_0 \mathcal{P}_a^2 + B_0 \mathcal{P}_b^2 + C_0 \mathcal{P}_c^2,$$

$$\mathcal{P}_i = \frac{\lambda_{ai} I_\alpha}{I_a} \mathcal{P}_a + \frac{\lambda_{bi} I_\alpha}{I_b} \mathcal{P}_b,$$

$$F = \frac{\hbar}{8\pi^2 I_\alpha} \frac{r}{r^2 - q^2},$$

$$r = 1 - \frac{\lambda_{ai}^2 I_\alpha}{I_a} - \frac{\lambda_{bi}^2 I_\alpha}{I_b} \quad (i = 1 \text{ or } 2),$$

$$q = -\frac{\lambda_{a1} \lambda_{a2} I_\alpha}{I_a} - \frac{\lambda_{b1} \lambda_{b2} I_\alpha}{I_b},$$

$\lambda_{\gamma i}$ = direction cosines between principal inertia axis γ ($\gamma \triangleq a, b, c$) and the internal rotation axis of i -th top ($i = 1, 2$).

$$\lambda_{a1} = -\lambda_{a2} = \cos(\theta) \quad (\text{see Fig. 2}),$$

$$\lambda_{b1} = \lambda_{b2} = \sin(\theta),$$

$I_a, I_b, I_c \triangleq$ principal moments of inertia,

I_α = moment of inertia of the SiH₃-top about its symmetry axis which is assumed to coincide with the internal rotation axis.

$\mathcal{P}_a, \mathcal{P}_b, \mathcal{P}_c \triangleq$ components of the overall angular momentum about the a -, b -, and c -principal inertia axis respectively.

$W_{v_i, \sigma_i}^{(n)}; W_{v_i, \sigma_i}^{(d)}$ = perturbation sums from perturbation treatment within the torsional states [12].

$$\begin{aligned} \mathcal{H}_{iD} &= \frac{1}{2} [[\mathcal{P}_i, \mathcal{H}_r], \mathcal{P}_i] \\ &= \mathcal{P}_i \mathcal{H}_r \mathcal{P}_i - \frac{1}{2} \mathcal{H}_r \mathcal{P}_i^2 - \frac{1}{2} \mathcal{P}_i^2 \mathcal{H}_r; \\ &\quad (i = 1, 2). \end{aligned}$$

\triangleq Stelman's denominator correction to the internal rotation perturbation sums [13].

$$\begin{aligned}\mathcal{H}_{\text{CD}} &= -D_J' \mathcal{P}^4 - D_{JK}' \mathcal{P}^2 \mathcal{P}_a^2 - D_{K'}' \mathcal{P}_a^4 \\ &\quad - \delta_J [\mathcal{P}^2 (\mathcal{P}_b^2 - \mathcal{P}_c^2) + (\mathcal{P}_b^2 - \mathcal{P}_c^2) \mathcal{P}^2] \\ &\quad - 2R_6' [3(\mathcal{P}_b^2 \mathcal{P}_c^2 + \mathcal{P}_c^2 \mathcal{P}_b^2) - \mathcal{P}_b^4 - \mathcal{P}_c^4] \\ &\triangleq \text{centrifugal distortion Hamiltonian;} \\ \mathcal{P}^2 &= \mathcal{P}_a^2 + \mathcal{P}_b^2 + \mathcal{P}_c^2; \\ &\triangleq \text{square of the overall angular momentum.}\end{aligned}$$

We note that the torsional part of Eq. (1) is based on a potential for the internal rotation $V(\alpha_1, \alpha_2)$ which may be described by simple three fold barriers i.e. by

$$\begin{aligned}V(\alpha_1, \alpha_2) &= \frac{V_3}{2} (\cos(3\alpha_1) - 1) \\ &\quad + \frac{V_3}{2} (\cos(3\alpha_2) - 1).\end{aligned}$$

Since at present our computer programs did not allow us to fit internal rotation parameters, rotational constants, and centrifugal distortion constants simultaneously, we did proceed as follows.

First centrifugal distortion was neglected and initial values for the rotational constants, A , B , C and the internal rotation parameters V_3 , I_α and θ were fitted to the absolute frequencies and to the torsional splittings given in Table 4 (the result was published in Ref. [9]). In the second step the centrifugal distortion constants were obtained from the AA-species spectrum. For the AA-species ($v_i = 0$, $\sigma_i = 0$; $i = 1, 2$) $W_{v_i, \sigma_i}^{(1)}$ and $W_{v_i, \sigma_i}^{(3)}$ are zero) and within the approximation of Eq. (1) the spectrum may be reproduced by a rigid rotor Hamiltonian plus corrections which are all of fourth order in the angular momentum operators:

$$\begin{aligned}\mathcal{H}_{\text{AA}} &= \overbrace{(A + 2a^2 F W_{0,0}^{(2)})}^{A_{\text{AA}}} P_a^2 \\ &\quad + \overbrace{(B + 2b^2 F W_{0,0}^{(2)})}^{B_{\text{AA}}} P_b^2 + C P_c^2 \\ &\quad + F W_{0,0}^{(4)} (\mathcal{P}_1^4 + \mathcal{P}_2^4) + \\ &\quad + W_{0,0}^d (\mathcal{H}_{1D} + \mathcal{H}_{2D}) + \mathcal{H}_{\text{CD}}\end{aligned}$$

Table 2. Effective rotational constants, centrifugal distortion constants, and correlation matrix for the AA-torsional substate of (SiH₃)₂S. The quoted uncertainties (in brackets) give one standard deviation as obtained in a least square fit.

A_{AA} [MHz]	9543.346 (9)	1.000								
B_{AA} [MHz]	2852.534 (2)	0.030	1.000							
C_{AA} [MHz]	2308.506 (2)	0.013	0.636	1.000						
D_J' [kHz]	2.116 (25)	-0.077	0.864	0.781	1.000					
D_{JK} [kHz]	-13.39 (24)	0.597	-0.227	-0.154	-0.375	1.000				
$D_{K'}$ [kHz]	60.7 (17)	0.829	0.086	-0.010	0.011	0.177	1.000			
δ_J [kHz]	0.651 (8)	-0.167	0.563	-0.154	0.386	-0.459	0.025	1.000		
R_6' [kHz]	0.012 (9)	0.459	-0.090	-0.032	-0.230	0.696	0.263	-0.486	1.000	

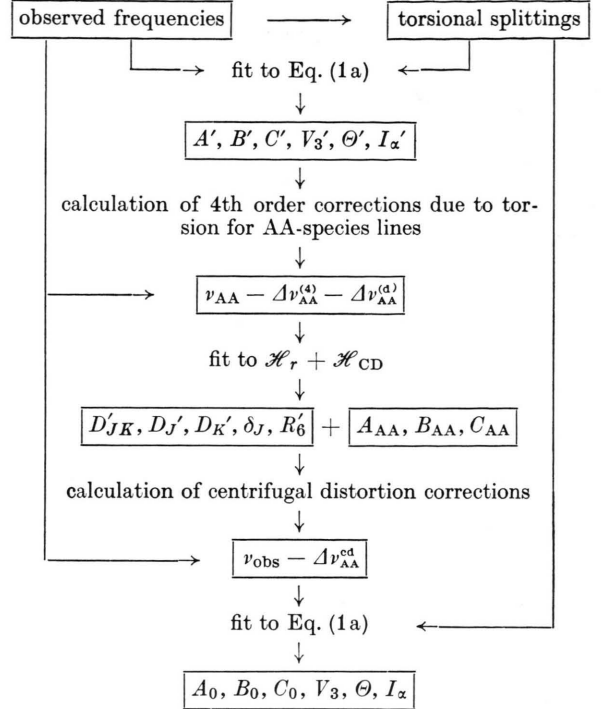


Fig. 1. Flowchart showing the fitting procedure followed in the analysis of observed frequencies and torsional splittings in the microwave spectrum of Disilylsulfide.

with

$$a^2 = \frac{\lambda_{ai}^2 I_\alpha}{I_a^2}, \quad b^2 = \frac{\lambda_{bi}^2 I_\alpha}{I_b^2} \quad (i = 1, 2).$$

With the approximate values for the rotational constants and internal rotation parameters, the fourth order corrections to the frequencies which arise from internal rotation i.e. from

$$F \sum_{i=1}^2 W_{0,0}^{(4)} \mathcal{P}_i^4 + \sum_{i=1}^2 W_{0,0}^d \mathcal{H}_{iD}$$

were calculated and subtracted from the observed frequencies. The so corrected frequencies were then

Table 3. Rotational constants and internal rotation parameters as used in Eq. (1); correlation matrix for the torsional groundstate of (SiH₃)₂S (conversion factor 505391 MHz amu Å²).

<i>A</i> [MHz]	9533.058 (9)	1.000						
<i>B</i> [MHz]	2851.927 (2)	−0.151	1.000					
<i>C</i> [MHz]	2308.507 (2)	0.257	0.317	1.000				
<i>V</i> ₃ [cal/mol]	522.6 (4)	0.258	−0.282	0.660	1.000			
<i>Θ</i> [°]	39.176 (28)	0.160	−0.208	−0.069	−0.215	1.000		
<i>I</i> _α [amu Å ²]	6.219 (6)	−0.302	0.334	−0.662	−0.976	0.017	1.000	
Derived constants: <i>F</i> [MHz] 89106 (82); <i>s</i> 27.339 (7).								

subjected to a standard centrifugal distortion treatment. The result is given in Table 2.

In the final step the centrifugal distortion contributions obtained for the AA-species were also used for EA, EE and AE species. Since the rotational Eigenfunctions of Eq. (1) are essentially the Eigenfunctions of *H*_R with some species dependent mixing of the *K*-doublet functions due to terms linear in *P*_a (if present) and since the asymmetric top expectation values for *P*_a² and *P*_a⁴ are essentially the same for the *K*-doublets, this simplified treatment is justified for Disilylsulfide, where the centrifugal distortion contributions due to *δ*_J and *R*_g' are sufficiently small.

After subtraction of the centrifugal distortion corrections (column 2 in Table 4) from the fre-

Table 4 (continued)

	<i>ν</i> _{obs}	<i>Δν</i> ^(cd)	obs.- calc.	<i>ν</i> _{AA} − <i>ν</i>	obs.- calc.
AE	24958.243		0.010	13.612	−0.003
EA	24956.250		−0.089	15.605	0.096
4 ₀₄ −4 ₁₃ AA	10057.436	−0.131	0.015		
EE	10048.088		0.034	9.348	−0.019
4 ₁₄ −5 ₀₅ AA	20564.595	−1.216	0.010		
EE	20568.424		0.080	−3.829	−0.070
AE	20571.167		0.066	−6.572	−0.056
EA	20572.814		−0.310	−8.219	0.320
4 ₀₄ −5 ₁₅ AA	28959.651	−0.169	−0.005		
EE	28953.149		−0.006	6.503	0.001
AE	28947.369		0.011	12.282	−0.016
EA	28945.892		−0.052	13.759	0.057
5 ₀₅ −5 ₁₄ AA	11866.767	−0.504	0.044		
EE	11855.826		0.032	10.941	0.012
5 ₁₅ −5 ₂₄ AA	25068.430	−0.337	0.045		
EE	25035.115		0.185	33.315	−0.140
5 ₁₄ −5 ₂₃ AA	18031.020	0.523	0.037		
EE	18019.494 ^a		−0.544	11.526 ^a	0.581
5 ₁₅ −6 ₀₆ AA	26202.074	−1.935	−0.003		
EE	26204.730		0.064	−2.656	−0.067
AE	26206.618		0.067	−4.544	−0.070
EA	26208.045		0.066	−5.971	−0.069
5 ₀₅ −6 ₁₆ AA	32873.143	−0.336	0.001		
EE	32867.449		−0.005	5.694	0.006
AE	32862.333		0.015	10.810	−0.014
EA	32861.185		−0.019	11.958	0.020
6 ₀₆ −6 ₁₅ AA	14214.806	−1.306	0.004		
EE	14201.916		0.000	12.890	0.004
AE	14188.884		0.056	25.922	−0.052
EA	14189.141		−0.082	25.665	0.086
6 ₁₆ −7 ₀₇ AA	31710.112	−2.757	−0.022		
EE	31711.750		0.050	−1.638	−0.072
AE	31712.839		0.078	−2.727	−0.100
EA	31713.900		0.110	−3.788	−0.132
6 ₀₆ −7 ₁₇ AA	36792.952	−0.636	−0.005		
EE	36788.065		−0.009	4.887	0.004
AE	36783.635		0.010	9.317	−0.015
EA	36782.723		−0.023	10.229	0.018
7 ₀₇ −7 ₁₆ AA	17126.820	−2.722	0.008		
EE	17111.486		0.004	15.334	0.004
AE	17095.956		0.035	30.864	−0.027
EA	17096.332		−0.093	30.488	0.101
7 ₁₆ −7 ₂₅ AA	17398.704	1.092	0.023		
EE	17383.018		−0.369	15.686	0.392
AE	17363.805		−0.015	34.899	0.038
EA	17372.520		0.182	26.184	−0.159
8 ₀₈ −8 ₁₇ AA	20579.236	−4.887	−0.002		
EE	20560.979		−0.011	18.257	0.009
AE	20542.424		0.009	36.812	−0.011
EA	20542.925		−0.199	36.311	0.197

Table 4. Microwave spectrum of (SiH₃)₂S in the torsional ground state (all frequencies in MHz). *Δν*^(cd) gives the contribution of the centrifugal distortion term [Eq. (1b)] to the transition frequencies. The torsional splittings of the rotational transitions (*ν*_{AA} − *ν*) are measured relative to the AA-species. ^anot included in the fit.

	<i>ν</i> _{obs}	<i>Δν</i> ^(cd)	obs.- calc.	<i>ν</i> _{AA} − <i>ν</i>	obs.- calc.
0 ₀₀ −1 ₁₁ AA	11852.301	−0.040	0.111		
EE	11840.166		−0.301	12.135	0.412
1 ₀₁ −2 ₁₂ AA	16470.740	−0.025	0.029		
EE	16461.610		−0.102	9.130	0.131
1 ₁₁ −2 ₂₀ AA	31511.677	−0.687	0.041		
1 ₁₀ −2 ₂₁ AA	30937.127	−0.681	0.040		
2 ₁₂ −3 ₀₃ AA	9178.022	−0.256	−0.041		
EE	9184.959		0.129	−6.937	−0.170
2 ₀₂ −3 ₁₃ AA	20830.205	−0.035	−0.007		
EE	20822.143		−0.029	8.062	0.022
AE	20815.580		0.009	14.625	−0.016
EA	20812.525		−0.163	17.680	0.156
3 ₀₃ −3 ₁₂ AA	8782.115	−0.009	−0.038		
EE	8720.135		0.054	7.980	−0.092
3 ₁₃ −3 ₂₂ AA	22533.682	−0.524	0.032		
EE	22465.684		−0.008	67.998	0.040
AE	22486.852		−0.033	46.830	0.065
EA	22361.197		0.075	172.485	−0.043
3 ₁₃ −4 ₀₄ AA	14861.831	−0.647	−0.025		
EE	14867.037		0.095	−5.206	−0.120
3 ₀₃ −4 ₁₄ AA	24971.855	−0.079	0.007		
EE	24964.578		0.009	7.277	−0.002

quencies, the corrected frequencies together with the splittings were used to fit simultaneously the final values for the rotational constants A , B , C and internal rotational parameters V_3 , I_α and θ . The results are shown in Table 3.

Table 4 gives the observed frequencies together with the calculated values, which are calculated by the use of Eq. (1 a, b) from the centrifugal distortion constants of Table 2 and the rotational constants and internal rotation parameters of Table 3.

The Molecular Electric Dipolemoment

The molecular Stark effect has been measured for the transition $1_{10} \rightarrow 2_{21}$ and $2_{02} \rightarrow 3_{13}$ of the AA species. The value of the electric dipolemoment $|\mu_b| = 0.896 \pm 0.008$ Debye was determined from a least squares fit to the observed Stark shifts listed in Table 5. The rotational energy differences involved in the second order Stark energy calculation, were obtained using the effective rotational constants A_{AA} , B_{AA} and C_{AA} of Table 2. The spectrometer was calibrated using OCS with $\mu = 0.71521$ Debye as standard [14].

Table 5. Stark satellites of the $1_{10} \rightarrow 2_{21}$ and $2_{02} \rightarrow 3_{13}$ rotational transitions of the AA torsional substate ($\Delta M_J = 0$).

	V/cm^a	$\pm M_J$	$\Delta\nu$ [MHz]	obs.-calc. [MHz]
$1_{10} \rightarrow 2_{21}$	742	0	1.433	— 0.023
	635	0	1.132	0.069
	744	1	— 2.675	— 0.047
$2_{02} \rightarrow 3_{13}$	635	0	— 1.295	0.020
	582	0	— 1.085	0.020
	1692	1	— 1.335	0.106
	1478	1	— 1.065	0.035
	635	2	3.158	0.025

^a The uncertainty in the electric field calibration is $\pm 0.2\%$.

The r_0 -Structure of Disilyldisulfide

Under the assumption of C_{3v} -symmetry for the SiH_3 groups there are five independent structural parameters (see Figure 2). These are the bond distances r_{SiSi} and r_{SiH} , the bond angles $\angle \text{SiSSi}$ and $\angle \text{HSiH}$, and the angle between the internal rotation axes (C_3 -axes) of the two silyl tops.

In analogy to the situation encountered in Dimethylether and Dimethylsulfide C_{2v} symmetry was also assumed for the most stable configuration

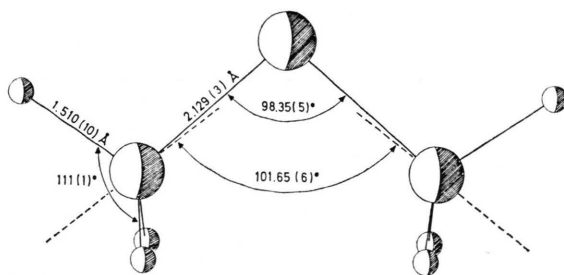


Fig. 2. r_0 -structure of Disilylsulfide as determined from a least squares fit to the rotational constants A_0 , B_0 , C_0 and internal rotation parameters θ and I_α listed in Table 3. C_{3v} symmetry of the SiH_3 -groups about their internal rotation axis was assumed and allowance was made for a small tilt of the internal rotation axes with respect to the Si—S bonds. Also assumed is the doubly eclipsed configuration of the two tops. This configuration has been determined to be the equilibrium structure for $(\text{CH}_3)_2\text{S}$.

when drawing Figure 2. Actually the orientation of the silyl tops i.e. the equilibrium values for the internal rotation angles α_1 and α_2 , remains undetermined by the present work, but we plan to determine them uniquely by an investigation of the spectra of partially deuterated molecules. Taking the rotational constants A_0 , B_0 , C_0 and the internal rotation parameters θ and I_α we have also five experimentally determined constants, which allow us, to fit to them a full r_0 -structure as shown in Figure 2. The agreement between the structural data as determined in the electron diffraction work [15] and the ones determined here is good. We note however, that there remain rather big discrepancies between the observed rotational constants and the values recalculated within a rigid rotor model from the above determined structural parameters (see Table 6).

This is most striking for the C -rotational constant and appears to be typical for this class of molecules.

Table 6. Comparison of the rotational constants of $(\text{SiH}_3)_2\text{S}$ as calculated from the r_0 -structure (see Fig. 2), with the experimental values (all in MHz). For comparison we give the corresponding values for $(\text{CH}_3)_2\text{S}$ from Ref. [2].

	obs.	calc.	obs.-calc.
A	9533.058	9532.858	0.200
B	2851.927	2848.131	3.796
C	2308.507	2318.550	— 10.043
for $(\text{CH}_3)_2\text{S}$:			
A	17810.0	17815.0	— 5.0
B	7621.0	7662.4	— 41.4
C	5717.8	5747.9	— 30.1

(For comparison the corresponding values for (CH₃)₂S are also given in Table 6.) This may indicate deficiencies of the theoretical model but it certainly also reflects the fact that the observed rotational constants are vibrational expectation values rather than rigid rotor values. The underlying problem becomes also apparent if one tries to calculate the moment of inertia of the silyl tops from the observed rotational constants. If the Si—S—Si frame and the silyl tops could be treated as rigid bodies I_α would be given by the following relation:

$$I_\alpha = \frac{1}{2}(I_{aa} + I_{bb} - I_{cc}) \\ = \frac{h}{8\pi^2} \left(\frac{1}{A} + \frac{1}{B} - \frac{1}{C} \right). \quad (2)$$

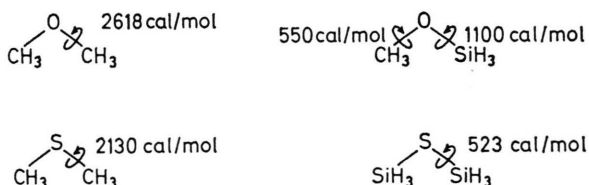
If one uses the rotational constants of Table 3 to calculate I_α according to Eq. (2) one obtains $I_\alpha = 5.64973(2) \text{ amu } \text{\AA}^2$, as compared to the directly determined value of $I_\alpha = 6.219(6) \text{ amu } \text{\AA}^2$. In the light of this result, some older investigations which in their analysis of the torsional splittings relied on the validity of Eq. (2) should be reviewed critically. Although the deviations between observed and calculated rotational constants are apparently big, it has been found for (CH₃)₂S, that the differences between r_0 - and r_s -bond distances are smaller than 0.01 Å. We think that this holds for (SiH₃)₂S as well.

Discussion

At the end of this work we contentedly noted that the Hamiltonian of Eq. (1) gave a really good fit to the observed spectrum (see Table 4), although the barrier to internal rotation is very low ($V_3 = 522.6 \text{ cal/mol}$). The limitation for the PAM Hamiltonian we use seems to lie at s -values below 10 [16].

The bond angle at the central sulfur atom observed here ($\angle \text{Si—S—Si} = 98.35^\circ$) is found to be nearly equal to the one observed for (CH₃)₂S ($\angle \text{C—S—C} = 98.9^\circ$) [2]. Contrary to Disilyl-ether/Dimethylether, where the corresponding bond angles differ considerably ($\angle \text{Si—O—Si} = 145^\circ$) [5], ($\angle \text{C—O—C} = 124^\circ$) [1], no such effect is observed here. This has been interpreted [15] in terms of a partial double bond character ($p\pi$ - $d\pi$ bonding) being present in the Si—O bond of (SiH₃)₂O but not in the Si—S bond of (SiH₃)₂S.

If, on the other hand, the electric dipole moments of (CH₃)₂S ($\mu_b = 1.551 \text{ D}$ [2]) and (SiH₃)₂S ($\mu_b = 0.896 \text{ D}$) are compared, it is realized that, although the difference in the electronegativities of silicon and sulfur is bigger than the one of carbon and sulfur and although the bond distance $r(\text{Si—S})$ is bigger than $r(\text{C—S})$, the observed dipole moment is smaller for (SiH₃)₂S. This effect is observed in all comparisons between silyl- and their homologous methylcompounds (as e.g. $\mu(\text{SiH}_3\text{Br}) = 1.318 \text{ D}$ [17], $\mu(\text{CH}_3\text{Br}) = 1.797 \text{ D}$ [18]) and is generally explained by assuming $p\pi$ - $d\pi$ bonding to be present in Silylcompounds. In the following we shall discuss the barrier to internal rotation. Since the barrier to internal rotation was not known for a Si—S bond so far, it is difficult to make any



comparisons. In a group of related molecules the relatively low value of the barrier observed here is noticeable.

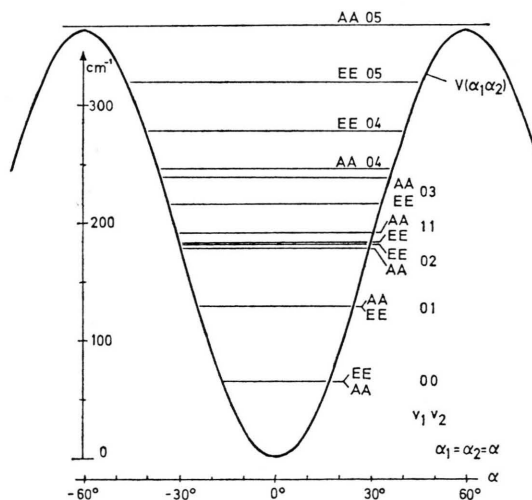


Fig. 3. Energy level scheme for the torsional vibration of (SiH₃)₂S as determined from torsional splittings of ground state rotational transitions in the microwave spectrum. The levels are characterized by the vibrational quantum numbers (v_1, v_2) of the two internal rotors and the symmetry species of the torsional wavefunction. For greater perspicuity the EA and AE levels are not included in this diagram. The torsional transition $(0, 0) \rightarrow (0, 1)$ of (SiH₃)₂S, which has not been observed so far, should be found near 63 cm^{-1} in the IR-spectrum.

Using the experimental data given in Table 3 it becomes possible to construct the energy level diagram for the torsional vibration of $(\text{SiH}_3)_2\text{S}$ (see Figure 3).

We are now able to predict the first torsional transitions to lie around 63 cm^{-1} $((0, 0) \rightarrow (0, 1))$ and 112 cm^{-1} $((0, 0) \rightarrow (0, 2))$ in the IR- and Raman spectrum.

Wir danken dem Fonds der Chemischen Industrie für die Gewährung eines Promotionsstipendiums für Karl-Friedrich Dössel. Darüberhinaus sei der

Deutschen Forschungsgemeinschaft und dem Fonds der Chemischen Industrie für die Bereitstellung von Sachmitteln gedankt. Herrn Prof. Dr. H. Dreizler danken wir für seine Unterstützung bei den MW-MW-Doppelresonanzexperimenten, durch die die aufgrund der Frequenzlagen und Starkeffektmuster ursprünglich getroffene Zuordnung des Rotationsspektrums abgesichert wurde, sowie für die Durchsicht des Manuskripts.

Die Rechnungen wurden auf dem PDP-10-Computer des Rechenzentrums der Universität Kiel durchgeführt.

- [1] P. H. Kasai and R. J. Myers, *J. Chem. Phys.* **30**, 1096 (1959).
U. Blukis, P. H. Kasai, and R. J. Myers, *J. Chem. Phys.* **38**, 2753 (1963).
H. Lutz and H. Dreizler, *Z. Naturforsch.* **31a**, 1026 (1976).
- [2] L. Pierce and M. Hayashi, *J. Chem. Phys.* **35**, 479 (1961).
H. Dreizler and H. D. Rudolph, *Z. Naturforsch.* **17a**, 712 (1962).
A. Trinkaus, H. Dreizler, and H. D. Rudolph, *Z. Naturforsch.* **28a**, 750 (1973).
- [3] J. F. Beecher, *J. Mol. Spectry.* **21**, 414 (1966).
G. K. Pandey and H. Dreizler, *Z. Naturforsch.* **31a**, 357 (1976).
G. K. Pandey, H. Lutz and H. Dreizler, *Z. Naturforsch.* **31a**, 1413 (1976).
- [4] H. Dreizler, *Fortschr. Chem. Forsch.* **10**, 59 (1968).
- [5] A. Almenningen, O. Bastiansen, V. Ewing, K. Hedberg, and M. Traetteberg, *Acta Chem. Scand.* **17**, 2455 (1963).
- [6] J. R. Durig, M. J. Flanagan, and V. F. Kalasinsky, *J. Chem. Phys.* **66**, 2775 (1977).
- [7] H. J. Emeléus, A. G. MacDiarmid, and A. G. Maddock, *J. Inorg. Nucl. Chem.* **1**, 194 (1955).
- [8] C. Glidewell, *J. Inorg. Nucl. Chem.* **31**, 1303 (1969).
- [9] K.-F. Dössel and D. Sutter, *Z. Naturforsch.* **33a**, 500 (1978).
- [10] L. Pierce, *J. Chem. Phys.* **34**, 498 (1961).
- [11] B. P. van Eijk, *J. Mol. Spectry.* **53**, 246 (1974).
- [12] Tables of the perturbation coefficients by M. Hayashi and L. Pierce are reproduced in App. 12 of "Rotational Spectroscopy and Molecular Structure" by J. Wollrab, Academic Press, New York 1967.
- [13] D. Stelman, *J. Chem. Phys.* **41**, 2111 (1964).
- [14] J. S. Muenther, *J. Chem. Phys.* **48**, 4544 (1968).
- [15] A. Almenningen, K. Hedberg, and R. Seip, *Acta Chem. Scand.* **17**, 2264 (1963).
- [16] T. Naito, O. Ohashi, and I. Yamaguchi, *J. Mol. Spectry.* **68**, 32 (1977).
- [17] K.-F. Dössel and D. Sutter, *Z. Naturforsch.* **32a**, 1444 (1977).
- [18] R. G. Shulman, B. P. Dailey, and C. H. Townes, *Phys. Rev.* **78**, 145 (1950).
- [19] K.-F. Dössel, Ph. D. Thesis, Kiel 1978.